



Supplement of

Assessing urban methane emissions using column-observing portable Fourier transform infrared (FTIR) spectrometers and a novel Bayesian inversion framework

Taylor S. Jones et al.

Correspondence to: Taylor S. Jones (tsjones@bu.edu)

The copyright of individual parts of the supplement might differ from the article licence.

S1 Slanted Total Column Footprints

In order to create total column STILT footprints, model particles were released at altitudes of 25, 50, 75, 100, 150, 200, 300, 400, 600, 800, 1000, 1500, 2000, and 2800 meters relative to the instrument location. The latitude and longitude of the particle release were adjusted based on the solar zenith and azimuth angles at the time of the release. 1000 particles were released from each level.

The total column air number density is calculated as:

$$n_{total} = \frac{p_0 N_A}{g_0 M_{air}} \quad (S1)$$

where p_0 is air pressure at the surface, N_A is the Avogadro constant, g_0 is column-averaged standard gravity, and M_{air} is the average molar mass of air (0.29 kg/mol).

10 The weighting factor for the footprint from a particle release at altitude z is calculated as:

$$w(z) = \frac{n(z) \Delta z}{n_{total}} \quad (S2)$$

where $n(z)$ is the air number density at altitude z , and Δz is the thickness of the layer.

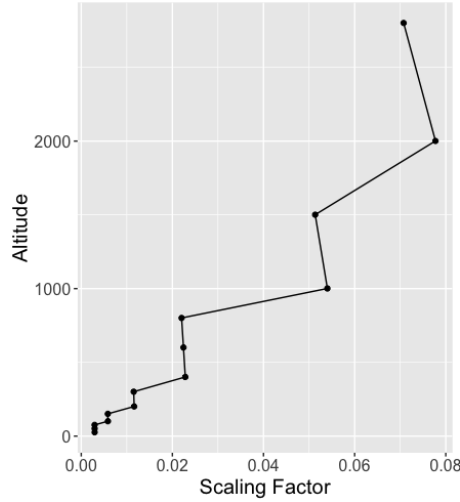


Figure S1. Pressure weighting scaling factors for each release height. Altitude values are in meters.

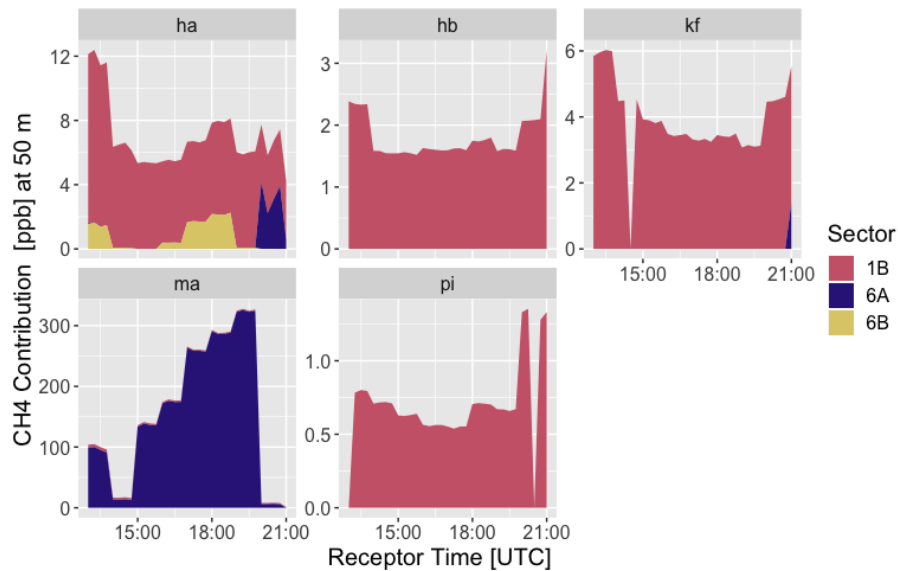


Figure S2. 50m footprints convolved with the prior emissions inventory. Expected enhancements at 50 m are on the order of 10 times the enhancement expected in the total column.

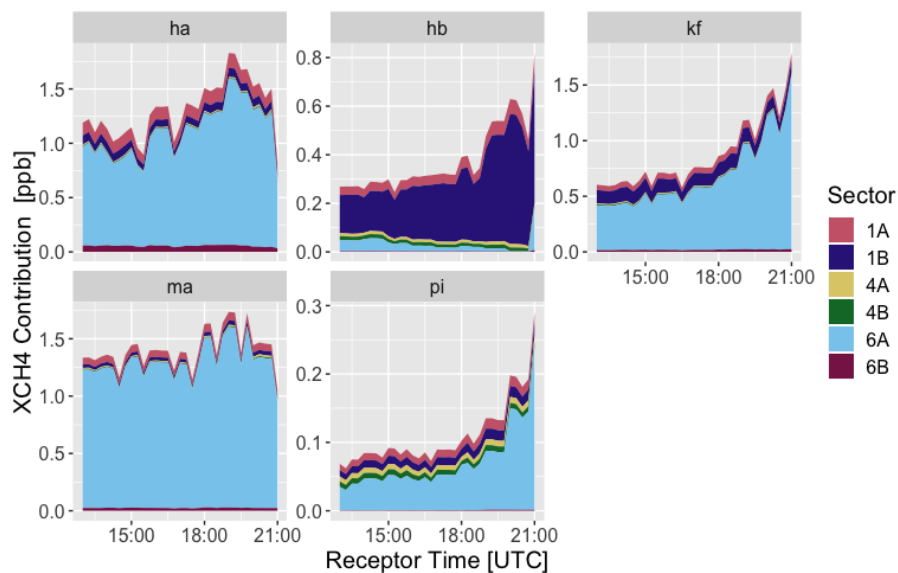


Figure S3. Total column footprints convolved with the EPA inventory. Notice that the landfill (6A) is present at additional sensors, this is because the emission is spread across a larger (10 km x 10 km) grid cell. This highlights the importance of using fine high-resolution inventories and giving special consideration to point sources.

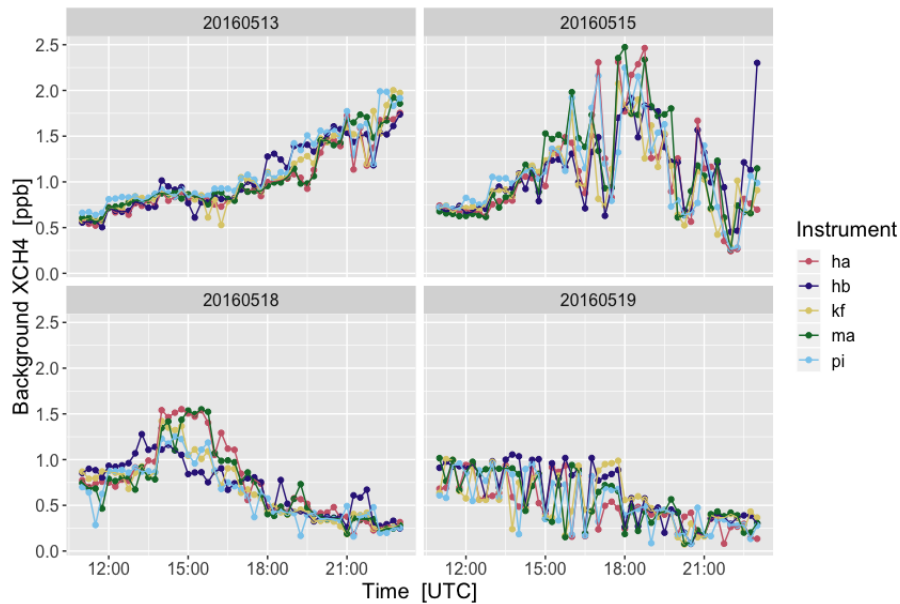


Figure S4. Enhancements in the regional background concentration seen by each sensor site. This was created using the EPA national gridded inventory and STILT footprint analysis using the NAM12km meteorological product.

S2 24-hour Background Simulation

- 15 Simulations using STILT footprint analysis and the EPA national gridded methane inventory show that the total column background concentration can be expected to vary more than one part-per-billion over the course of a day (Figure S4) due to continental emissions upwind. It is important to note that these values do not include the majority of the background methane (> 1.8 ppm), which is not attributable to emissions immediately upwind.

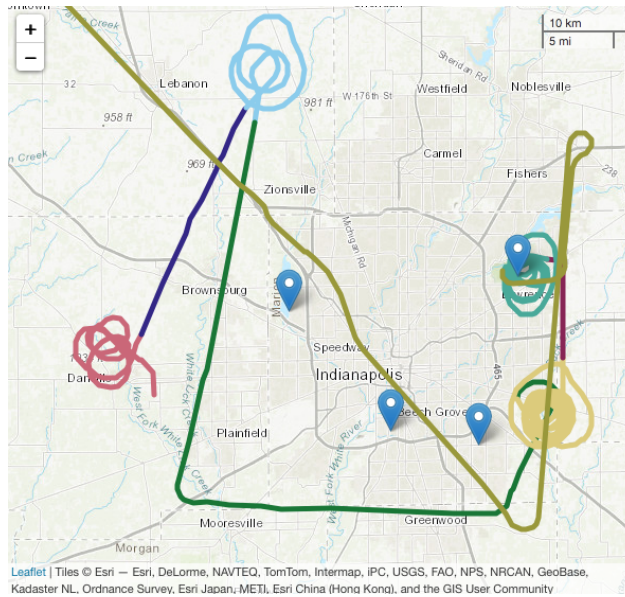


Figure S5. Flight path for the afternoon of May 13, 2016. The colors represent different sections of of the flight plan, which included four spirals at different points around the city.

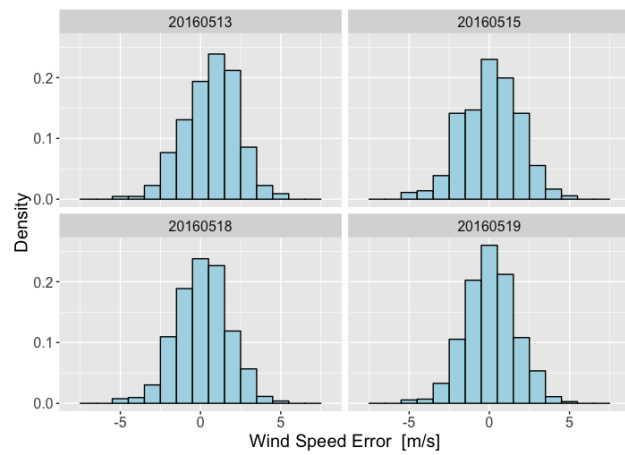


Figure S6. Distributions of wind speed error (model - measurement) for each flight throughout the campaign.

S3 Wind Error Calculations

In order to assess the uncertainty in the wind speed and direction values in the NAM-12km model, independent aircraft measurements were analyzed. An example flight path from one of these flights is shown in Figure S5. The distributions of difference between measured and model wind speed are shown in S6.

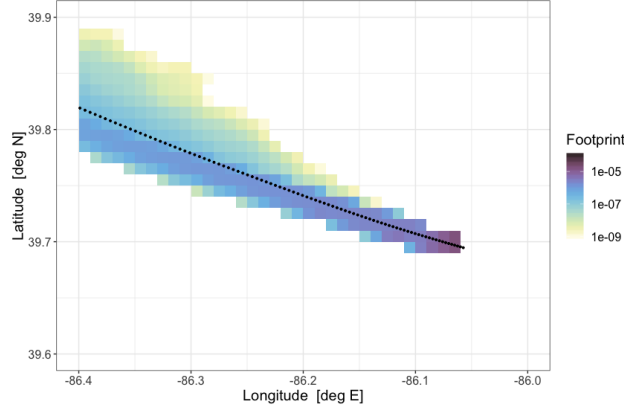


Figure S7. Footprint with no added transport error. The mean trajectory is shown in black.

S4 Transport Error Calculations

In order to determine the effect of transport error, we begin with several assumptions:

1. The two errors that affect transport are errors in horizontal wind speed (w_s) and wind direction (w_d)
- 25 2. Both errors can be characterized as having a normal distribution with known variances (σ_{ws}^2 and σ_{wd}^2) and are auto-correlated with respect to time, with known time scales (T_{ws} and T_{wd}).
3. Wind speed and directions are completely correlated with respect to distance. This is an acceptable assumption because the domain of interest is small (≈ 100 km by 100 km) compared to reported error correlation length scales of meteorological products.
- 30 4. Wind errors are also completely correlated at all relevant altitudes.

The mean wind speed, $w_s(t)$, and direction, $w_d(t)$, can be extracted from the mean particle positions at each time step ($\bar{x}(t)$, $\bar{y}(t)$).

$$w_s(t) = \frac{d}{dt} \sqrt{\bar{x}^2(t) + \bar{y}^2(t)} \quad (\text{S3})$$

$$w_d(t) = \frac{d}{dt} \tan^{-1} \left(\frac{\bar{x}(t)}{\bar{y}(t)} \right) \quad (\text{S4})$$

- 35 An example footprint, along with mean particle positions at each time step are shown in Figure S7. We can draw a sample time series for the wind speed error distribution, ε_{ws} . An example is in figure S8. A sample from the wind direction error distribution ($\varepsilon_{wd}(t)$) can also be drawn (Figure S9)

$$\delta_x = (w_s + \varepsilon_{ws}) \sin(w_d + \varepsilon_{wd}) - w_s \sin(w_d) \quad (\text{S5})$$

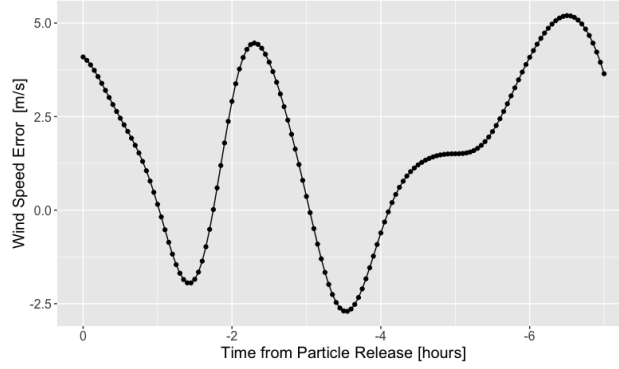


Figure S8. Example wind speed error time series, $\varepsilon_{ws}(t)$, for a particle release going back 7 hours.

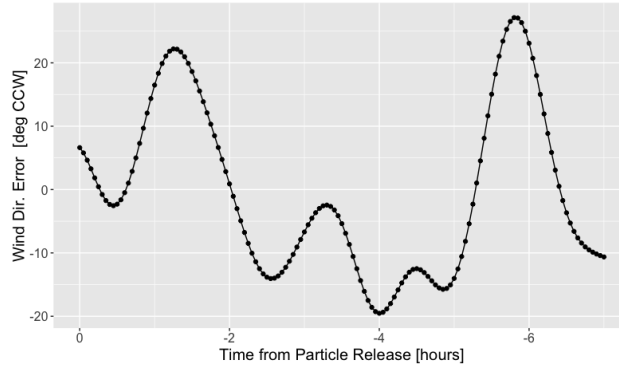


Figure S9. Example wind direction error time series, $\varepsilon_{wd}(t)$, for a particle release going back 7 hours.

$$\delta_y = (w_s + \varepsilon_{ws}) \cos(w_d + \varepsilon_{wd}) - w_s \cos(w_d) \quad (\text{S6})$$

- 40 The cumulative ground distance (Δx and Δy) that must be added to each particle at any point in time is the accumulation of the error movements since the release time ($t = 0$).

$$\Delta x(t) = \int_t^0 \delta x(\tau) d\tau \quad (\text{S7})$$

$$\Delta y(t) = \int_t^0 \delta y(\tau) d\tau \quad (\text{S8})$$

These cumulative displacements are shown in Figure S10

- 45 Figure S7 shows a footprint for a receptor at an altitude of 51 m, where 1000 particles were moved backwards in time for 7 hours. Figure S11 shows a footprint from the same STILT simulation, however each particle's ground position has been shifted every minute to reflect the cumulative wind errors $\Delta x(t)$ and $\Delta y(t)$.

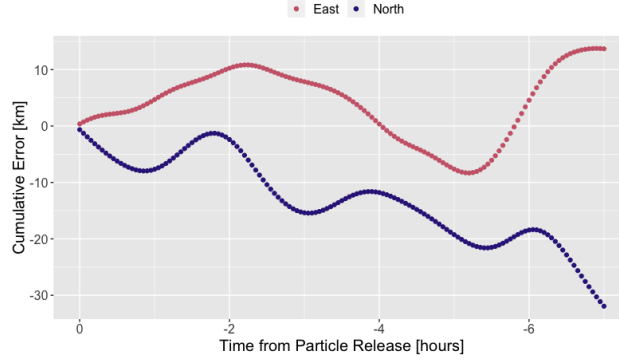


Figure S10. Cumulative displacement in both the latitudinal ($\Delta y(t)$) and longitudinal ($\Delta x(t)$) directions.

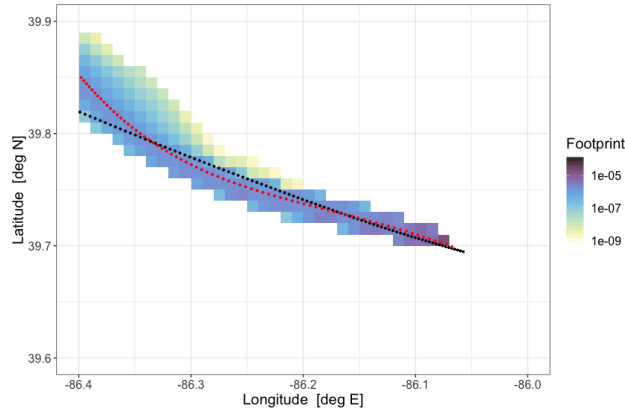


Figure S11. Footprint with added transport error. The adjusted mean transport is shown in red, while the original mean transport is in gray.

When the footprint with no added error is multiplied by the prior emissions field, and the contributions from each grid cell added together, this represents the concentration (in ppb) expected at the receptor. When this is done with the footprint with error, there will be a resulting error in the expected concentration.

If this process is repeated a large number of times, each time drawing new time series for $\varepsilon_{ws}(t)$ and $\varepsilon_{wd}(t)$, the resulting distribution of enhancements will represent the distortion of the true model result due to transport errors. The results of 400 simulations at each of the release altitudes are shown in Figure S12.

The errors from each height can be combined using the same pressure weighting scaling factors, $w(z)$, as the footprints:

$$\sigma_{mod}^2 = \sum_{i=1}^L w(z_i) \sigma_{mod}(z_i)^2 \quad (\text{S9})$$

Standard Error at each altitude, and the cumulative error in the column from the ground are shown in Figure S13. The value of σ_{mod} is 0.25 ppb.

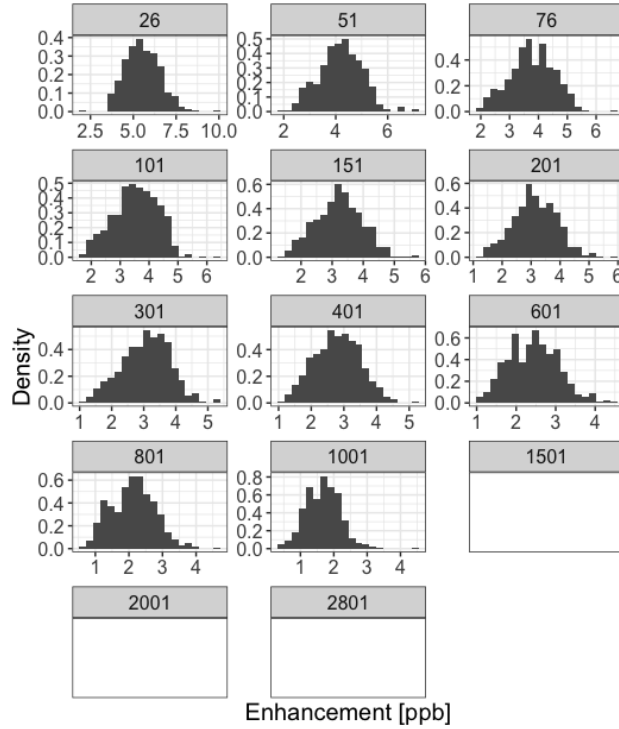


Figure S12. Density of Enhancements for 400 error simulations at each particle release level.

S5 Background Parameter Sensitivity Analysis

In order to test how sensitive our inversion results were, we tested different combinations of values for the background prior variance (FIND) and background time scale (t_{back}). Figure S14 shows the result of this test.

This analysis shows that the inversion results are sensitive to the order of magnitude of these two parameters, but that small changes in these choices would not drastically affect the inversion output. Even though the exact values chosen for these parameters are not critical, this analysis shows that incorporating the background into the inversion itself does change the results. For instance, if an extremely low background prior variance was chosen, the posterior emission rate would be several times higher ($> 300 \text{ Gg yr}^{-1}$) which would not be realistic. This would be equivalent to using a fixed background value that is subtracted out before the inversion. Also, the background time scale has an important effect on the posterior error, because it proscribes how correlated all of the posterior background values must be. If this value is too small, then the background would be able to vary greatly between adjacent time steps, which increases the degrees of freedom and can result in over-fit.

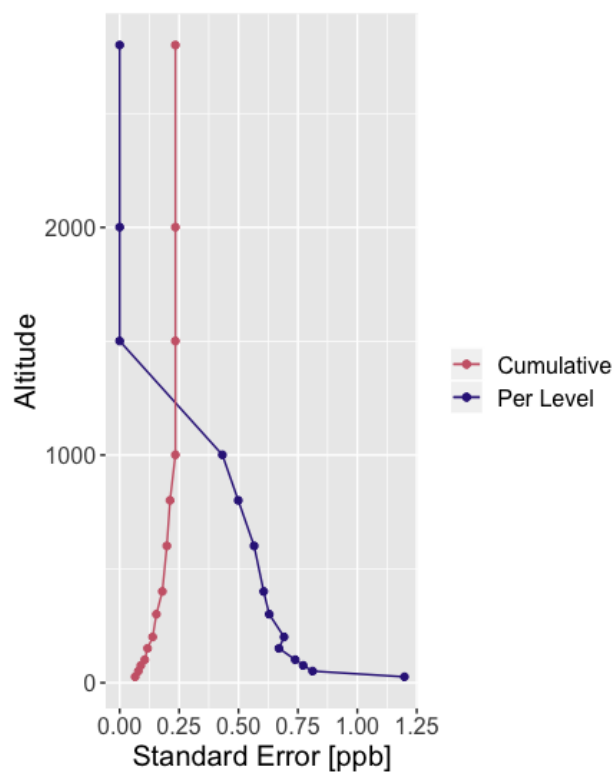


Figure S13. Standard error by particle release height and cumulative standard error. The blue points represent the standard deviations of the distributions shown in Figure S12, while the red points represent the cumulative sum of these values after being weighted with scaling factors $w(z)$.

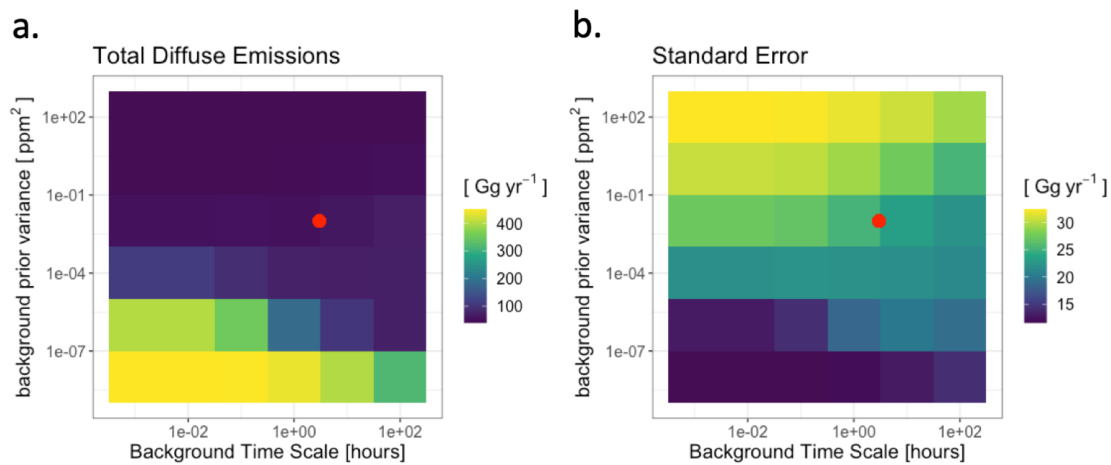


Figure S14. The posterior total diffuse methane emissions (a) and corresponding posterior error (b) calculated using different combinations of values background prior variance and background time scales. The red point indicates the values used throughout the paper. Note that both the x- and y-axis values are on logarithmic scales, as several orders of magnitude were tested.